JOURNAL OF MATERIALS SCIENCE **39** (2004) 1437– 1440

Static and dynamic fracture toughness of epoxy/alumina composite with submicron inclusions

P. R. MARUR, R. C. BATRA, G. GARCIA, A. C. LOOS
Department of Engineering Science and Mechanics, MC 0219 Virginia Polytechnic Institute and State University, Blacksburg, VA 24061, USA
E-mail: rbatra@vt.edu

The influence of the particle size and the volume fraction of submicron spherical alumina particles in an epoxy matrix on the fracture toughness of the composite is investigated experimentally. Three particle sizes, 50 nm, 500 nm and 5 μm are used. The static and the dynamic fracture toughnesses are evaluated from the 3-point bend tests. It is found that the particle size significantly affects the static and the dynamic fracture toughness.

Particulate composites with either nanosize particles or carbon nanotubes as reinforcements are getting increased attention because of the expectation of orders of magnitude improvement [1] in their strength and elastic moduli over conventional reinforcements. Niihara and coworkers [2, 3] have reported a dramatic increase in the mechanical performance of ceramic matrices containing ceramic nanoparticles. However, Todd *et al*. [4] and Cambier *et al*. [5] measured a modest increase in the fracture toughness of a nanocomposite over that of alumina, and Sternitzke *et al*. [6] found that the fracture toughness of a nanocomposite decreased. Warren *et al*.'s [7] work suggests that the deflection of the crack path is a key contributor to the toughening mechanisms in alumina composites. There appears to be no clear consensus on the effect of particle size, volume fraction of reinforcements and mechanisms influencing the toughness of nanocomposites.

For polymer matrix composites, a general trend is that the fracture toughness increases with an increase in the volume fraction of reinforcing particles before reaching a plateau at around 50% volume fraction [8]. Mechanisms contributing to the enhancement in the strength of particulate composites are the change in the fracture mode to transcrystalline, flaw size reduction due to smaller grains, crack deflection at inclusions, and crack bridging. Several investigations [2–4, 9] support the change in the fracture mode from intergranular to transgranular. For nanosize particles, the fracture may not be transgranular. For instance, Birringer *et al*. [10] found that nominally brittle materials become ductile at room temperature when the grain size is about 100 nm. Ash *et al*. [11] have reported a 400% increase in the ductility of 5 wt% nanophase alumina filled epoxy over that of pure epoxy.

The particulate composites were prepared by dispersing solid alumina particles in a slow curing epoxy EPOTHIN supplied by Buehler. Spherical alumina particles of mean diameters 50 nm (AKP-G008, Sumitomo Chemical Co., Japan), 500 nm (AKP-3000, Sumitomo Chemical Co., Japan) and 5000 nm (Buehler) were used as inclusions. Values of Young's modulus E, Poisson's ratio ν and mass density ρ for the epoxy (alumina) are 2.85 GPa (400 GPa), 0.36 (0.22) and 1149 kg/m^3 (3990 kg/m^3) respectively.

The epoxy is prepared by mixing 73.5 wt% of epoxy resin and 26.5% of hardener. The mixture is gently stirred for 10 min at room temperature and allowed to degas for 10 min. Then an appropriate quantity of alumina particles is added to the resin/hardener mixture which is again stirred slowly till particles have been uniformly mixed with the resin and air bubbles have escaped. The mixture is then poured carefully into a mold made of PMMA plates held together by four bolts. The edges of the mold are first lined with a cellophane tape and then coated twice with a polyurethane release agent to facilitate the separation of the specimen from the mold after curing at room temperature for 24 h. Thin sheets of the particulate composite are allowed to stabilize for at least seven days before they are cut and machined into rectangular test specimens. The initial plan was to fabricate composites with nominal volume fractions of 2%, 5%, 10%, 20% and 40% alumina particles. However, good quality specimens with a large volume fraction of smaller size alumina particles could not be prepared. Therefore, the maximum volume fractions of 500 nm and 50 nm alumina particles were limited to 30% and 10% respectively.

For each particle size and each volume fraction of the inclusions, five specimens were machined with the span (S)/width (W) and the crack-length (a)/width equal to 4 and 0.25 respectively. Edge notches were machined with a Buehler diamond wafer blade resulting in a nominal crack tip radius of 75 μm. For non-zero radius of the notch-root, the dependence of fracture toughness on the notch-root radius should be considered. However, no such relations are available for particulate composites with submicron size particles.

The static 3-point bend tests were performed in an Instron testing machine at a cross-head speed of 0.2 mm/min, and the load-displacement data was recorded. Fracture is assumed to initiate at the peak load P_c, and the fracture toughness, K_{Ic}, is computed

0022–2461

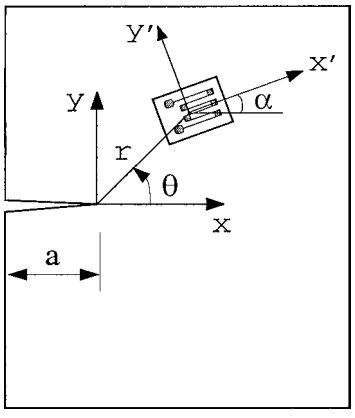

Figure 1 Location of a strain gage near a crack-tip.

from the relation [12]:

$$K_{\mathrm{Ic}} = \frac{SP_{\mathrm{c}}}{BW^{3/2}} \times \frac{3\lambda^{1/2}[1.99-\lambda(1-\lambda)(2.15-3.93\lambda+2.7\lambda^2)}{2(1+2\lambda)(1-\lambda)^{3/2}}; \quad \lambda = a/W, \tag{1}$$

where B is the specimen thickness.

The dynamic 3-point bend tests were conducted by using a specially designed drop weight tower. The stress intensity factor (SIF) is measured by using Dally and Sanford's [13] method of mounting a strain gage close to the crack tip. Referring to Fig. 1 the distance r is taken to be $0.6B$ to avoid the three-dimensional stress field around the crack-tip. Angles α and θ are computed from

$$\cos 2\alpha = -\frac{1-\nu}{1+\nu}, \quad \tan\frac{\theta}{2} = -\cot 2\alpha. \tag{2}$$

The axial strain, $\epsilon_{x'x'}$, in the uniaxial strain gage (CEA-13-032UW-120) is related to the SIF, K_{I}, through

$$K_{\mathrm{I}} = E\sqrt{2\pi r}\epsilon_{x'x'}/(1+\nu) \times \left(\eta\cos\frac{\theta}{2} - \frac{1}{2}\sin\theta\cos\frac{3\theta}{2}\cos 2\alpha + \frac{1}{2}\sin\theta\cos\frac{3\theta}{2}\sin 2\alpha\right). \tag{3}$$

The strain gage output is checked by statically loading the specimen to 50% of the static fracture load, P_{c}. It ensures proper gage bonding, lead wire connection and instrumentation settings.

Time histories of the tup force, the anvil reaction and the strain gage reading are used to analyze transient elastic deformations of the composite specimen by the finite element method (FEM). Owing to the symmetry of the geometry and the loads about the vertical centroidal axis of the specimen, deformations of one-half of the specimen are analyzed by using 4-node quadrilateral elements in the FE code ANSYS. Values of Young's modulus and Poisson's ratio computed from the test data of static tests are used in the FE model. We have compared in Fig. 2 the so computed time history of K_{I} with that obtained from Equation 3 and the strain gage data; the two are found to be close to each other.

The dependence of the dynamic fracture toughness, K_{Id}, of the composite upon the volume fraction of alumina for two different sizes of alumina particles is exhibited in Fig. 3; K_{Id} for the neat epoxy equals 1.4 MPa$\sqrt{m}$. For composites with 5 μm alumina particles, K_{Id} first increases with an increase in the volume fraction of alumina particles from 2% to 10% and subsequently essentially stays constant. However, the opposite trend is seen for composites with 500 nm alumina particles.

The static, K_{Ic}, and dynamic, K_{Id}, fracture toughness values for the composites with 5 μm and 500 nm size particles are compared in Fig. 4a and b. For 50 nm size particles, K_{Ic} and K_{Id} were found to equal 1.79 and 0.80 MPa$\sqrt{m}$ for 2% volume fraction, and 1.29 and 1.12 MPa$\sqrt{m}$ for 10% volume fraction of particles. In every case, the dynamic fracture toughness is significantly lower than the static fracture toughness. Nakamura *et al.* [14] have also reported a similar noticeable reduction in the fracture toughness with an increase in the strain rate

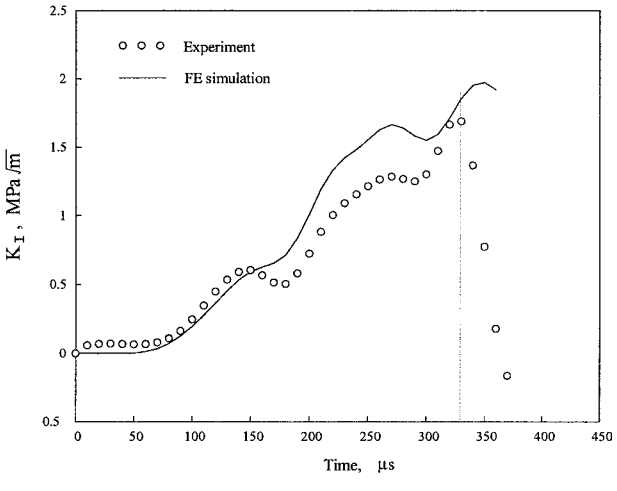

Figure 2 Comparison of the dynamic SIF for a sample from the FE simulations and the test data. Dotted line marks the time of fracture initiation.

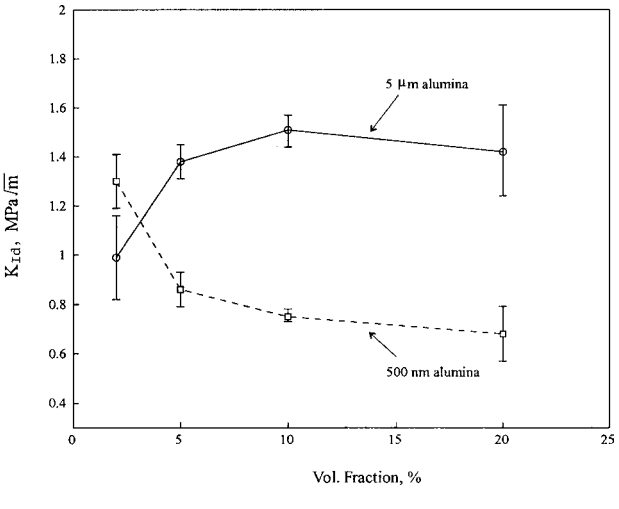

Figure 3 Dependence of the dynamic fracture toughness upon the volume fraction of alumina particles.

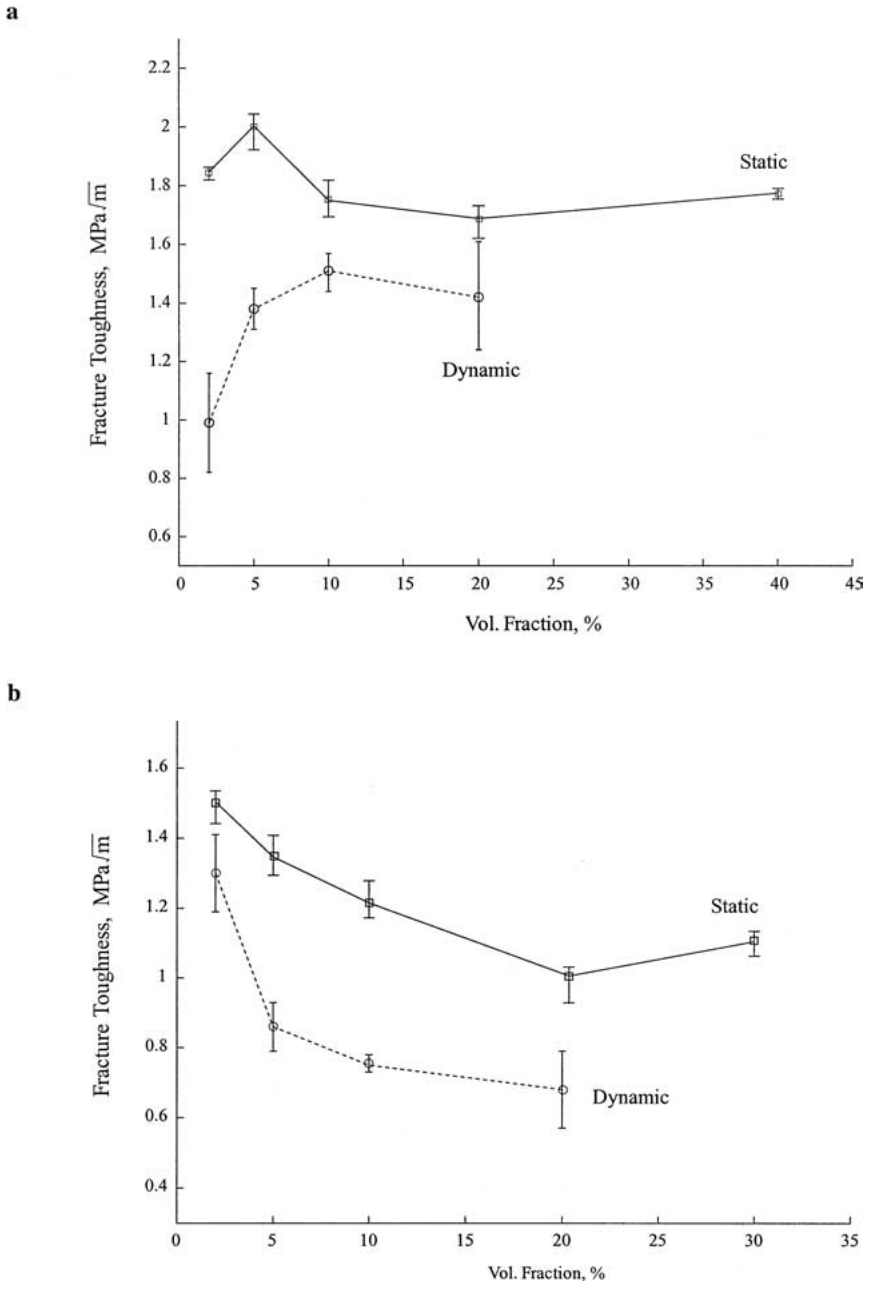

Figure 4 Comparison of static and dynamic fracture toughness values for composites with (a) 5 μm and (b) 500 nm alumina particles.

in epoxy resins reinforced with silica particles. Also, the dynamic fracture toughness was found to increase with an increase in the particle size.

The elastic moduli (results not reported here) are found to be essentially independent of the particle size but strongly depend upon the volume fraction of the alumina. For a given volume fraction of alumina particles, except for the 2% volume fraction, smaller size particles reduce the dynamic fracture toughness. For the 5 μm size alumina particles, the dynamic fracture toughness first increases with an increase in the volume fraction of alumina particles, reaches a plateau and then decreases a little. However, for the 50 nm and 500 nm size particles, the dynamic fracture toughness decreasses with an increase in the volume fraction of the reinforcements. For both 500 and 5000 nm alumina particles, the static fracture toughness is higher than the dynamic fracture toughness for the same volume fraction of inclusions.

Acknowledgments

This work was supported by the ONR grant N00014-98-1-0300 to Virginia Polytechnic Institute and State University and the AFOSR MURI grant to Georgia Tech which awarded a subcontract to Virginia Polytechnic Institute and State University.

References

1. Z. REN, E. T. THOSTENSON and T. W. CHOU, *Comp. Sci. Technol.* **61** (2001) 1899.
2. K. NIIHARA and A. NAKAHIRA, in Proceedings of the Third International Symposium on Ceramic Materials and Components for Engines, edited by V. T. Tennery (American Ceramic Society, Westerville, OH, 1988) p. 919.
3. K. NIIHARA, *J. Ceram. Soc. Japan* **99** (1991) 974.
4. R. I. TODD, C. E. BORSA, S. JIAO and R. J. BROOK, *J. Microscopy* **177** (1994) 305.
5. F. CAMBIER, M. POORTEMAN, A. LERICHE, D. O'SULLIVAN, S. HAMPSHIRE, R. W. DAVIDGE, R.

J. BROOK and T. KENNEDY, *J. Eur. Ceram. Soc.* **16** (1996) 799.
6. M. STERNITZKE, L. CARROLL and B. DERBY, *Acta Materiallia* **44** (1996) 4543.
7. R. WARREN, T. HANSSON and J. WASEN, *J. Hard Mater.* (1994) 00.
8. C.-E. ROUSSEAU and H. V. TIPPUR, *Acta Materialia* **48** (2000) 4021.
9. J. LLORCA, M. ELICES, P. MIRANZO, J. PEREZ-RIGUEIRO, J. Y. PASTOR and J. S. MOYA, *ibid.* **46** (1998) 5399.
10. R. BIRRINGER, J. KARCH and H. GLEITER, *Nature* **330** (1987) 556.
11. B. J. ASH, J. STONE, P. M. AJAYAN, R. W. DOREMUS, R. W. SEIGEL, S. K. CHANG and L. S. SCHADLER, *Scripta Materialia* **44** (2001) 2061.
12. J. E. SRAWLEY, *International Journal of Fracture* **12** (1976) 475.
13. J. W. DALLY and R. J. SANFORD, *Experimental Mechanics* **27** (1988) 381.
14. M. OKUBO, Y. NAKAMURA, M. YAMAGUCHI and T. MATSUMOTO, *Polymer* **33** (1992) 3415.

Received 16 June
and accepted 16 September 2003